TAILORING SPIN EXCITATIONS BY NANOLITHOGRAPHY

BY DIRK GRUNDLER, FABIAN GIESEN, AND JAN PODBIELSKI

Spintronics devices [1] made from metallic thin films have already been successful for a decade. They are based on multilayers of magnetic and nonmagnetic material. Patterned by nanolithography, such multilayered devices have revealed novel spin dynamics properties. In particular, spin precession and ferromagnetic resonance (FMR) were observed driven by a dc current. At the same time magnons, i.e., spin excitations with finite wave vector k, have been argued to form a basis for further magnetoelectronics applications [2]. Here tailoring, manipulation and interference of spin waves are of central importance. These features constitute the emerging field of magnonics. Large progress in studying spin dynamics in nanopatterned magnets has been achieved in recent years. We review experiments on spin wave excitation in ferromagnetic rings [3-8], which might present building blocks of magnonics. We outline the current understanding of spin wave discretization and localization. In particular, we show how spin excitations can be tailored by both the geometrical confinement due to nanolithography and the inhomogeneous internal field H_{int}. H_{int}, which includes the external, demagnetizing and effective exchange field is essential for the spin dynamics.

BROADBAND SPIN WAVE SPECTROSCOPY

Experimental data were obtained on a series of samples prepared from polycrystalline $Ni_{80}Fe_{20}$ (permalloy). This ferromagnetic material was advantageous as it did not exhibit intrinsic magnetic anisotropy. Each sample contained an array of nominally identical rings [Fig. 1(a)]. From sample to sample, the width w of the rings was varied systematically between 300 and 950 nm. The outer diameter was kept constant at 2.1 μm. The thickness t was about 15 nm to ensure that spins were preferentially in the plane of the magnetic film. To measure the spin wave dynamics over the frequency regime from 45 MHz to 20 GHz the rings were integrated on coplanar wave

SUMMARY

There is a great interest in spin excitations in nanostructured solids. For semiconductor solids a major driving source is spintronics, i.e., the concept of using not only the charge but also the spin state of an electron for information processing. For magnetic nanosystems, collective spin excitations and spin waves are intriguing as they might form the basis for magnonics.

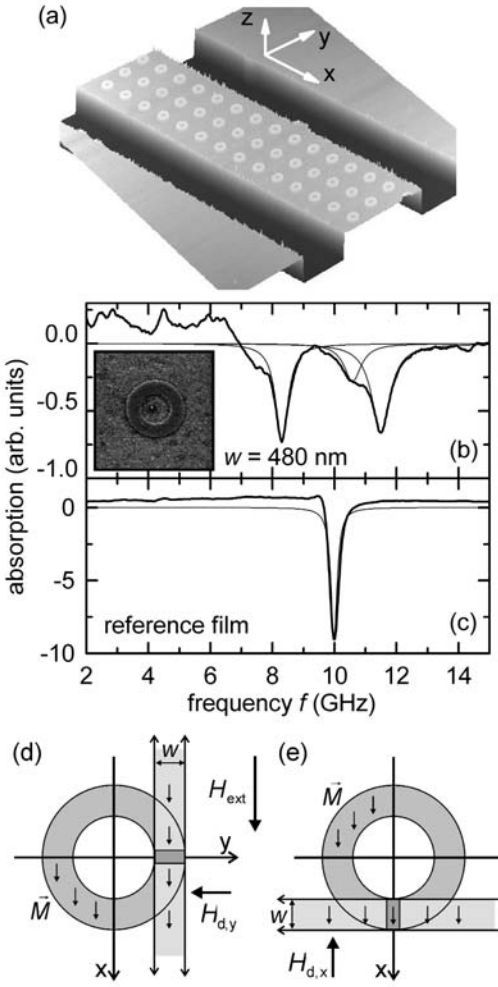

Fig. 1 **(a) Atomic force micrograph of a coplanar wave guide with integrated ferromagnetic rings.** The width of the central conductor is 15μm. The thickness of the rings is 15 nm. (b) Absorption spectrum for $Ni_{80}Fe_{20}$ rings with $w = 480$ nm (cf. scanning electron micrograph) at $\mu_0 H_{ext} = 90$ mT applied along the coplanar wave guide (x direction). Lorentz curves highlight spin wave eigenfrequencies. (c) Ferromagnetic resonance of the $Ni_{80}Fe_{20}$ reference film at 90 mT. Sketches in (d) and (e) compare the onion state of rings with a wire which is magnetized along and perpendicular to its axis, respectively.

Dirk Grundler <grundler@ph.tum.de>, Fakultät für Physik E10, Technische Universität München, D-85748 Garching, Germany.

Fabian Giesen, Max-Born-Institut, Max-Born-Str. 2A, D-12489 Berlin, Germany.

Jan Podbielski, Institut für Angewandte Physik, Universität Hamburg, Jungiusstr. 11, D–20355 Hamburg, Germany

guides [3]. We investigated several arrays, each containing between 15 and several hundreds of rings. The exact number determined the signal-to-noise ratio but not the spin wave excitations. Frequency-resolved power absorption was measured by a commercial broadband vector network analyzer at different *fixed* external magnetic fields H_{ext}. The sinusoidal high-frequency magnetic field $\vec{h}_{hf}$ surrounded the central conductor and was mainly in the plane of the rings. The torque between the magnetization $\vec{M}$ and $\vec{h}_{hf}$ excited spin precession and the spin waves. Varying H_{ext} and the magnetic history, we controlled $\vec{M}$ and the domain configuration of the rings: (i) at large H_{ext} we generated the so-called onion state. Here, both ring halves (ring arms) were magnetized in parallel and domain walls existed at the head and tail. (ii) At small H_{ext} we induced the reversal, and the so-called vortex state was formed. At remanence this intriguing state did not exhibit a stray field as microscopic magnetic moments were aligned with the ring perimeter. For information storage one aims at realizing a clockwise or counterclockwise circulation direction of spins.

In Fig. 1(b) we show an absorption spectrum of rings in the onion state at $\mu_0 H_{ext} = 90$ mT. The rings have a width of 480 nm. We summarize the main experimental findings: (I) Two main modes exist, one at high frequency (mode A) and one at low frequency (mode B). (II) In between there is a satellite mode with weak intensity. In narrow rings we resolve up to four satellite modes. We compare these data with an unpatterned $Ni_{80}Fe_{20}$ reference film deposited in the same run. In Fig. 1(c) we observe only one pronounced resonance.

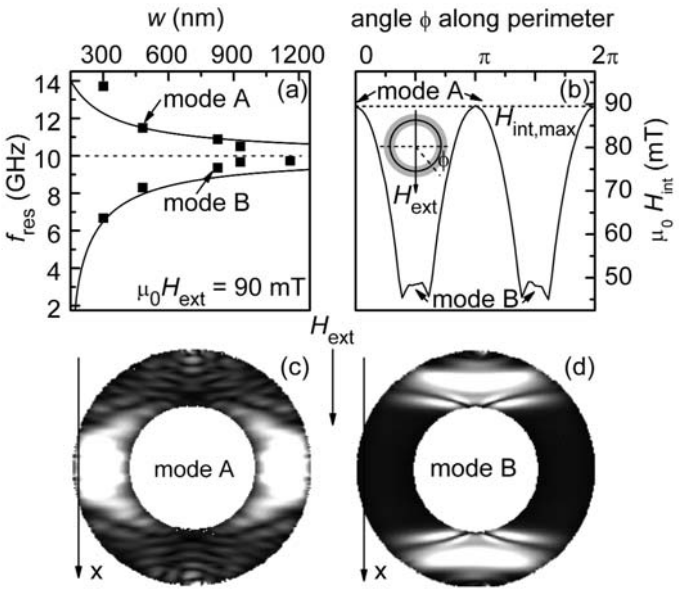

Fig. 2 **(a) Comparison between spin wave modes A and B** measured in rings and disks at 90 mT (full symbols) and calculated ferromagnetic resonances in wires (solid lines). For details see text. The broken line depicts the FMR in the reference film. (b) Sketch of the internal field (simulated) in the ring's onion state along the azimuthal direction ϕ. Graphs (c) and (d) depict simulated spin wave patterns for mode A and mode B, respectively. A field of 90 mT is applied along the *x* direction. Bright means large spin wave amplitude.

LOCALIZATION OF SPIN WAVES

For a thin film, Kittel calculated the resonance frequency a long time ago [9]. Since then the formalism is part of solid state physics textbooks. For the film it is assumed that all spins precess at the same frequency and that the wave vector k is zero. The uniform excitation is called FMR. Boundaries of the film introduce demagnetization fields H_d. These are large if spins point perpendicular to the edge and small if spins are parallel. Both types of demagnetization fields, i.e., static and dynamical fields, are relevant for the spin dynamics. For thin and infinitely long wires the Kittel formalism [9] predicts the following FMR eigenfrequency

$$f_{res} = \frac{\gamma\mu_0}{2\pi}\left(\left(H_{ext} + \left(N_y - N_x\right)M_S\right) \times \left(H_{ext} + \left(N_z - N_x\right)M_S\right)\right)^{\frac{1}{2}}. \quad (1)$$

Here, γ is the gyromagnetic ratio and M_s the saturation magnetization. For the in-plane direction we use the demagnetization factors N_x and N_y. N_z accounts for the direction perpendicular to the plane. The demagnetization factors for the center of a wire oriented along both the direction of the external field H_{ext} and the *x* axis are given by $N_x = 0, N_y = \frac{2t}{\pi w}, N_z = 1 - \frac{2t}{\pi w}$. [10] [$H_{ext}$ is applied in the *x* direction in Figs. 1(d) and (e).] The demagnetization factors N_y and N_z lead to positive prefactors of M_s in Eq. (1). By this means the internal field H_{int} becomes large and the precession frequency is increased with respect to an unpatterned film. For a wire oriented along the *y* axis, i.e., perpendicular to the magnetic field direction, N_x and N_y interchange: $N_x = \frac{2t}{\pi w}, N_y = 0, N_z = 1 - \frac{2t}{\pi w}$. In this case a negative prefactor results for M_s in Eq. (1). Consequently H_{int} is reduced. In Fig. 2(a) we depict these two eigenmodes of long permalloy wires as a function of *w* (full lines).

Strikingly, in Fig. 2(a) the main modes A and B of rings follow the two FMR modes calculated for wires of the same width which are magnetized in the two orthogonal directions, i.e., along and perpendicular to the wire axis. The dependence on *w* demonstrates that demagnetization fields due to the mesoscopic width are important for the measured spin wave eigenfrequency. By nanopatterning, we control f_{res}. Indeed, in the onion state of a ring two extreme spin orientations are present: in the ring arms spins are parallel to the ring's boundary and in the head and tails spins point perpendicular to the edges. This is illustrated in Figs. 1(d) and (e). We might interpret our devices as infinitely long wires which are bent to form a ring. The qualitative comparison with the Kittel formalism of wires already suggests that, due to an inhomogeneous internal field, spins in different ring segments precess at different eigenfrequencies. The spin excitation splits up into two (or more)

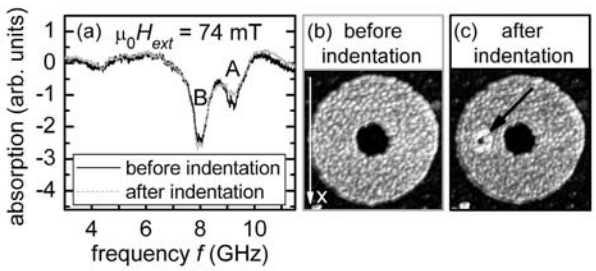

Fig. 3 **(a) Absorption spectra measured in the onion state** of 850 nm wide rings before (gray) and after (black) AFM nanolithography. (b) AFM picture of an as-prepared ring. (c) The same ring with a nanopit introduced by AFM lithography. The pit has a diameter of 100 nm and a depth of 10 nm.

modes. In the following we will discuss how local details of the internal field, the finite wave vector and the localization of spin waves are essential to understand the spin excitations in micromagnets. Micromagnetic simulations are powerful to illustrate these important aspects. Simulated data are shown in Figs. 2(b) to (d). The simulations are performed in a similar way to what has been done for rings in Refs. [7,8]. We find that the ring geometry together with the applied external field leads to an internal field profile that varies characteristically as a function of azimuthal direction ϕ [Fig. 2(b)]. Local maxima of H_{int} are found for ring segments which are magnetized in parallel with H_{ext} and local minima for the head and tails where spins point perpendicular to the edges. Interestingly, spin waves with negative group velocity, i.e., backward volume magnetostatic waves (BVMSW's), reside at maximum H_{int} [Fig. 2(c)], and spin waves with positive group velocity, i.e., Damon-Eshbach-like spin wave modes, become localized in the minima [Fig. 2(d)]. Outside these ring segments the corresponding spin waves do not exhibit a real wave vector and are damped. Such localization and discretization phenomena due to inhomogeneous magnetic fields form a research field of great current interest.

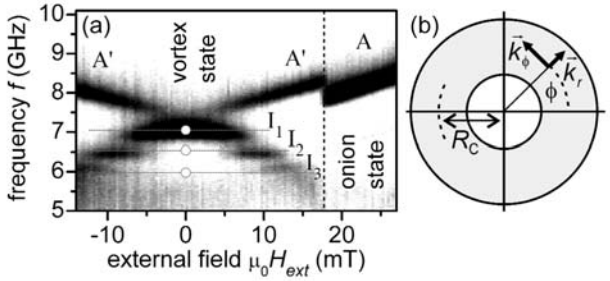

Fig. 4 **(a) Gray-scale plot of a series of absorption spectra** (adapted from Ref. 8) measured in the vortex state near $H_{ext} = 0$. The rings have a width of 600 nm. Dark represents high absorption due to spin wave excitation. The vertical line indicates the switching field where the rings enter the onion state for increasing H_{ext}. White filled circles depict calculated eigenfrequencies based on Eq. (2). Dashed horizontal lines are guides to the eyes. (b) Parameters used in the text.

NANOMANIPULATION

We have used the detailed knowledge of spin waves in rings to control them by nanomanipulation and by this means to substantiate the localization phenomenon. Let us focus again on the onion state. We have used an atomic force microscope (AFM) to introduce a nanopit in a specific ring segment [Figs. 3(b) and (c)] [11]. Intentionally the nanopit is in a segment where the ring's magnetization is in parallel with the magnetic field when applied along the *x* direction. Spectra obtained before and after nanomanipulation are shown in Fig. 3(a). The absorption strength of mode A is altered whereas the absorption strength of mode B remains unaltered. The experiment using AFM nanolithography thus underlines the localization of spin wave modes in rings. Furthermore it demonstrates that spin excitations can be tailored efficiently in a successive manner. Analyzing the spectra in detail we find that the nanopit leads to a reduction in absorption for mode A of a few 10% if related to one of the excited ring segments alone [cf. Fig. 2(c)].

MAGNONIC RING RESONATOR

Let us now address the vortex state of ferromagnetic rings. Here we consider rings without a nanopit. At remanence the internal field H_{int} is constant as a function of ϕ along the ring. Localization phenomena due to field inhomogeneities do not take place. This is in contrast to the onion state. When we investigate in detail the spin wave spectra of Fig. 4(a) obtained on 600 nm wide rings we find discrete eigenfrequencies as a function of magnetic field H_{ext}. They exhibit almost plateau-like values with frequency gaps in between. This behavior is contrary to the modes found in the onion state which show a monotonous dispersion as a function of H_{ext} [cf. mode A in Fig. 4(a)]. In the following we discuss the microscopic origin of the discrete eigenfrequencies I_n ($n = 1,2,..$) in the vortex state. It is useful to index the spin waves by the integer number of nodal lines *m* and *n* along the radial $\vec{e}_r$ and azimuthal $\vec{e}_\phi$ directions, respectively [Fig. 4(b)]. The total wave vector *K* is decomposed by $K^2 = k_r^2 + k_\phi^2$. In the radial direction discrete values $k_r = k_{mr}$ are obtained due to the geometric ring boundaries. Here, a quantization condition holds which is similar to the one of a longitudinally magnetized wire [12]. Important for our discussion is the azimuthal component k_ϕ which is parallel to the ring's magnetization and represents a BVMSW traveling around the ring. The spin excitations should exhibit a further quantization condition and should fulfill

$$n \cdot 2\pi = \oint k_\phi(f, H_{int}(\phi))\, r\, d\phi, \qquad (2)$$

where *r* is the radius of the integration path. Equation (2) is the condition for constructive interference and ensures that a spin wave exhibits the same phase after traveling around the ring. Starting from the formalism developed for a magnetic wire [13] and introducing periodic boundary conditions we are able to calculate eigenfrequencies based on Eq. (2) [8]. Symbols shown in Fig. 4(a) are for $r = R_C$ and $m = 0$. The discrete eigenfrequencies and the frequency gaps are remodeled rather well.

However, the calculated modes depicted as symbols exist at $H_{ext} = 0$, whereas we observe discrete modes I_n with $n \geq 2$ for $H_{ext} \neq 0$ in the experiment. Equation (2) does not include the specific excitation mechanism. In the experiment, the high-frequency field h_{hf} is homogeneous in the rings' plane. To excite BVMSW of high wave vectors $k_{n\phi}$ with $n \geq 2$, an inhomogeneous internal field H_{int} or a spatially inhomogeneous magnetization are needed. The inhomogeneity is generated by applying the external field which polarizes the vortex state. H_{int} becomes an oscillating function of ϕ and the perfect ring-like symmetry of $\vec{M}$ is broken. By this means, excitation of high k values becomes possible. Both to ensure a constant eigenfrequency f_{res} around the ring and to fulfill Eq. (2), the wave vector $k_\phi(\phi) = k_\phi(f, H_{int}(\phi))$ changes with ϕ through the variation of H_{int} [8]. This explains the small magnetic field dependence of the eigenfrequencies observed in the experiment. We have found that changing the width w modifies the discrete spin wave eigenfrequencies and the frequency gaps in a controlled way. A magnetic ring thus acts as a ring resonator for BVMSW.

By decentering the inner hole we achieved further control over the vortex state recently. We succeeded in generating the clockwise and counterclockwise circulation direction of spins in a deterministic manner [14]. If one decreases further both the geometrical width and ring diameter, exchange effects might play an increasingly important role for the spin excitations. Combined with nanomodifications using AFM lithography one would enter an intriguing regime for future magnonics investigations.

ACKNOWLEDGEMENTS

The authors gratefully acknowledge support of the work by B. Botters, D. Heitmann, and by M. R. Freeman for the possibility to perform dynamic micromagnetic simulations at the University of Alberta. We are thankful for the support of the German Excellence Initiative via the "Nanosystems Initiative Munich (NIM)" and the SFB 668 of the Deutsche Forschungsgemeinschaft.

REFERENCES

1. S. A. Wolf *et al*., *Science* **294**, 1488 (2001); D. Grundler, *Phys. World* **15** (4), 39 (2002).
2. R. Hertel *et al*., *Phys. Rev. Lett*. **93**, 257202 (2004).
3. F. Giesen *et al*., *Appl. Phys. Lett*. **86**, 112510 (2005).
4. F. Giesen *et al*., *J. Appl. Phys*. **97**, 10A712 (2005).
5. J. Podbielski *et al*., *Superlattices and Microstructures* **37**, 341 (2005).
6. X. Zhu *et al*., *J. Appl. Phys*. **99**, 08F307 (2006).
7. I. Neudecker *et al*., *Phys. Rev. Lett*. **96**, 057207 (2006).
8. J. Podbielski *et al*., *Phys. Rev. Lett*. **96**, 167207 (2006).
9. C. Kittel, *Phys. Rev*. **73**, 155 (1948).
10. R.I. Joseph and E. Schlömann, *J. Appl. Phys*. **36**, 1579 (1965).
11. J. Podbielski *et al*., unpublished.
12. C. Mathieu *et al*., *Phys. Rev. Lett.* **81**, 3968 (1998).
13. K.Y. Guslienko *et al*., *Phys. Rev. B* **68**, 024422 (2003).
14. F. Giesen *et al*., *Phys. Rev. B* **75**, 184428 (2007).